POLITECNICO MILANO 1863

SCUOLA DI INGEGNERIA INDUSTRIALE
E DELL'INFORMAZIONE

Executive Summary of the Thesis

A New Source-Sink Space Environment Evolution Model Including the Effects of Orbit Transfer Maneuvers

Laurea Magistrale in Space Engineering - Ingegneria Spaziale

Author: Davide Gusmini

Advisor: Prof. Pierluigi Di Lizia

Co-advisors: A. D'Ambrosio, S. Servadio, P. M. Siew, R. Linares

Academic year: 2022-2023

---

1. Introduction

The growing interest in space activity and the deployment of large satellite constellations, such as Space-X Starlink, Astra Space, and Amazon Kuiper, will significantly increase the number of satellites in Low Earth Orbit (LEO). The deployment of mega-constellations will affect satellites safety during orbit transfer maneuvers due to the risk of in-transit conjunction with other Anthropogenic Space Objects (ASO). Currently, space debris is the primary danger to operational satellites. Collisions between active satellites and space junk could create additional debris, causing a cascade effect known as the "Kessler Syndrome". Therefore, an accurate understanding of the space environment and its time evolution is necessary to promote space sustainability and to mitigate debris creation.

Two different methodologies are traditionally used to estimate the time evolution of the space environment's population: Monte Carlo (MC) and source-sink models. MC methods consider real physical dynamics and multiple perturbations, including atmospheric drag, solar radiation pressure, Earth's oblateness, third-body perturbations, space weather. These methods are highly accurate but computationally intensive and require multiple simulations to produce general statistics. Examples of MC models include LEGEND, DAMAGE, and DELTA.

On the other hand, source-sink models are based on a system of coupled Ordinary Differential Equations (ODEs) to describe the evolution of various ASO categories, including active and inactive payloads, rocket bodies, explosion and collision debris, which can interact with each other. This modeling approach is less detailed as it groups ASOs by species. Thus, it is computationally lighter and faster with respect to the MC approach, making it suitable for long-term predictions and sensitivity analyses, but it lacks the capability to follow individual objects. Nevertheless, these models are versatile and can accommodate various forms of discretization, such as species, orbital altitude, and physical characteristics (mass, area, and diameter).

Previous studies have already utilized source-sink models to study the LEO population For example, Somma et al. [1] introduced a feedback controller and developed the so-called MISSD (Model for Investigating control Strategies for Space Debris). This model was then used by Trozzi et al. [2] to analyze different definitions of orbital capacity. The current study utilizes an evolutionary multi-shell multi-species source-sink model belonging to the MIT Orbital Capacity Assessment Tool (MOCAT) family. This includes different source-sink versions already employed to analyze various aspects of the space environment's evolution and orbital capacity. D'Ambrosio et al. [3] developed the MOCAT-3 based on the model introduced in the report written by the US government's independent advisory body JASON. An extension with respect to the MOCAT-3 has been proposed by D'Ambrosio et al. [4] with the so-called MOCAT-4N, where the debris family is subdivided into two subgroups: trackable and untrackable debris. Other studies have examined orbital slotting, stability and system-level risk in the LEO environment, as well as the effects of launch rate distribution on source-sink model stability and LEO environmental capacity sensitivity to projected demand.

2. Objective

The thesis proposes an evolutionary multi-shell multi-species source-sink model belonging to the Massachusetts Institute of Technology (MIT) Orbital Capacity Assessment Tool (MOCAT) family. The model aims to achieve a more realistic simulation of the space environment by including rocket bodies and the upwards and downwards fluxes of objects due to orbit transfer maneuvers. The proposed model is a natural extension of D'Ambrosio et al work [3, 4]. Moreover, the thesis analyzes the implications of these maneuvers on the orbital capacity, it conducts a sensitivity analysis on critical parameters, such as the low-thrust acceleration magnitude and the number of satellites launched, and finally it determines, through an optimization algorithm, the optimal injection orbit altitude to maximize the number of satellites in orbit while minimizing debris.

3. Methodology

Source-sink models generally involve simplifying assumptions. [3] Indeed, previous versions of MOCAT models assumed that new active satellites are directly injected into their final operational altitude and, after the mean satellite lifetime, they are instantly removed from the simulation instead of performing maneuvers to lower their altitude. Given the high number of satellites planned to be launched, an upward flux of objects raising from the injection to the final operative altitude is expected. Analogously, a second downward flux of spacecraft lowering their altitude until they are burned up in the atmosphere will be formed. As a result, having a more realistic model capable of describing these flows of spacecraft performing orbit raising and deorbiting maneuvers becomes critical.

The proposed multi-bin multi-species source-sink model discretizes the LEO region by altitude and species. It does so by dividing the region into several orbital spherical shells, each with a thickness of 50 km, and categorizing the population into six distinct object classes: active satellites, further subdivided into three subcategories (raising S_r, operative S_h, and deorbiting S_d satellites), derelicts D, debris N, and rocket bodies B. Raising satellites represent spacecraft maneuvering from injection to operative orbit, operative satellites are those station-keeping and performing their mission tasks in their assigned operative altitude, and those re-entering the atmosphere at the end of their operational lifetime are referred to as deorbiting. The resulting population vector, altitude h and time t dependent, can be expressed as $\boldsymbol{P} = [S_h, S_r, S_d, D, N, B]$. The h and t dependence is omitted for clarity. A system of ordinary differential equations is utilized to describe the temporal evolution of the population vector $\boldsymbol{P}$, resulting in

$$\dot{\boldsymbol{P}} = \dot{\boldsymbol{\Lambda}} + \dot{\boldsymbol{C}}_{PMD} + \dot{\boldsymbol{C}} + \dot{\boldsymbol{F}} \tag{1}$$

Equation (1) includes terms related to new launches, Post-Mission Disposal (PMD), collisions, and other additional fluxes, represented by $\dot{\boldsymbol{\Lambda}}$, $\dot{\boldsymbol{C}}_{PMD}$, $\dot{\boldsymbol{C}}$, and $\dot{\boldsymbol{F}}$, respectively.

Figure 1 shows a schematic representation of the proposed MOCAT model. Three types of intact objects are considered: active satellites, rocket bodies, and derelicts. Collisions, black dashed arrows, can produce derelicts, debris, or both. The creation of derelicts from each active satellite category is indicated with red dotted arrows. Green arrows show the launch of both S_r and S_h, while the flow between different shells and category transitions are indicated with ϑ. The model considering $\boldsymbol{P} = [S_h, S_r, S_d, D, N, B]$ is named MOCAT-6RD, while MOCAT-4B is a simple model without orbit transfer fluxes, with $\boldsymbol{P} = [S, D, N, B]$.

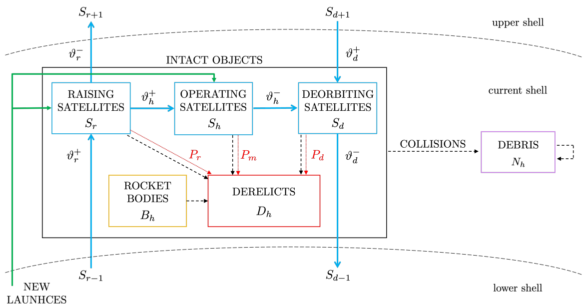

Figure 1: Schematics of the MOCAT-6RD.

3.1. New Launches

The launch rate, denoted as $\dot{\mathbf{\Lambda}}$, represents the number of objects launched per year. As the model considers that decaying satellites, derelicts, and debris are not launched, their corresponding $\lambda_{S_d,D,N}$ values are assumed to be zero. Additionally, it is assumed that all upcoming rocket bodies utilized for deploying active satellites will be reusable and will reenter the Earth's atmosphere after launch, resulting in $\lambda_B = 0$. Finally, the launch rate results in

$$\dot{\mathbf{\Lambda}} = [\lambda_{S_h}, \lambda_{S_r}, 0, 0, 0, 0] \tag{2}$$

The files provided by the International Telecommunication Union (ITU)[1] are used to determine the first two terms. To incorporate this data into the model, certain assumptions are necessary. Filters based on their altitude range (LEO region) and eccentricity (near-circular orbits) are applied. A feasibility percentage, representing a confidence level, is associated to each file entries. Moreover, the model assumes a deployment time of 10 years, during which the number of satellites launched follows the exponential trend fitting historical data. After 10 years, the number of launches becomes constant. In addition, the complete set of TLEs for Starlink and OneWeb was obtained from Space-Track[2] to determine the distribution of injection orbits.

3.2. Post-Mission Disposal

The Post-Mission Disposal (PMD) process accounts for the average operational lifetime of a satellite, represented by Δt. Upon reaching the end of their operational life, a fraction of active satellites is assumed to become derelict by failing to conduct PMD, consistent with the MOCAT-3 model. [3] Rather than being instantly removed from the simulation, the remaining active satellites transition from S_h to decaying satellites S_d and begin to descend in altitude. Therefore, the term $\dot{\boldsymbol{C}}_{PMD}$ can be formulated as:

$$\dot{\boldsymbol{C}}_{PMD} = \left[-\vartheta_h^-, 0, P_m\vartheta_h^-, (1-P_m)\vartheta_h^-, 0, 0\right] S_h \tag{3}$$

with P_m being the post-mission disposal probability of success and $\vartheta_h^- = 1/\Delta t$ represents the PMD transition. The first term in Eq. (3) is negative, as it involves the removal of operating satellites from the population S_h. A portion of those failing PMDs is transferred to the derelict population D, while the rest undergo successful disposal and are added to S_d.

3.3. Collisions

Collisions in the proposed model, similar to the MOCAT-3 model, are based on the kinetic theory of gases. [1, 3] The interactions are simplified by summing all active satellites within a specific shell, where $S = S_h + S_r + S_d$. Additionally, all active satellites are assumed to have the same collision avoidance capability regardless of their operational phase (raising, station keeping, or deorbiting). The term for collisions, $\dot{\boldsymbol{C}}$, can be expressed as follows:

$$\dot{\boldsymbol{C}} = [\dot{C}_S, \dot{C}_D, \dot{C}_N \cdot n_f, \dot{C}_B] \tag{4}$$

where n_f represents the number of fragments generated by a collision between object i and j. It is estimated with the NASA Standard Breakup Model (SBM). [5] The proposed model assumes that collisions involving active satellites, derelicts, and rocket bodies are catastrophic, while those involving debris are non-catastrophic.

3.4. Atmospheric Drag Flux

The flux of objects decaying into lower altitude shells due to atmospheric drag, represented by $\dot{\boldsymbol{F}}_d$, affects all families except for active satellites, which are assumed to be capable of performing station-keeping maneuvers. Thus, for active satellites, $\dot{F}_{d,S} = 0$. The flux is modeled as in the MOCAT-3 model, and for the generic species Q, it is given by:

$$\dot{F}_{d,Q} = -\frac{Q_+ v_+}{d} + \frac{Qv}{d} \tag{5}$$

[1] `https://www.itu.int`
[2] `https://www.space-track.org`.

The thickness of the shells is assumed constant and indicated by d, while the rate of change of the semi-major axis is denoted by v and it is computed as $v = \dot{a} = -\rho B_c \sqrt{\mu a} \approx -\rho B_c \sqrt{\mu R}$. Being a the semi-major axis, μ the Earth's gravitational parameter, ρ the atmospheric density, R the orbital radius, and B_c the ballistic coefficient. The subscript $+$ denotes the upper shell, while its absence refers to the current shell. Note that due to the negative sign in the definition of v, the first term of Eq. (5) represents the influx of objects into the current shell, while the second term represents the outflux of objects leaving the current shell.

3.5. Orbit Transfer Flux

The flux resulting from orbit transfer maneuvers is modeled in this work by taking into account the secular variation of the semi-major axis $\bar{a}(t)$ under the influence of a low-thrust acceleration vector of magnitude ϵ. According to Di Carlo and Vasile [6], it can be expressed as

$$\bar{a}(t) = \left[\frac{1}{\bar{a}_0} + C_1 t^2 - C_2 t\right]^{-1} \tag{6}$$

being C_1 and C_2 two constant whose value depend on the low-thrust acceleration ϵ, the initial semi-major axis $\bar{a}_0$, and other parameters.
The diagonal matrix $\mathbf{T} = \text{diag}(\tau_{ot_h})$ collects the time that satellites spend in each shell during the orbit transfer maneuvers. After being injected into the parking orbits, raising satellites initiate an increase in their altitude. As the launched batch leaves the current to enter into the upper shell, a certain number of satellites, whose final operational altitude is within the current shell, are deposited. The deposition is described by the diagonal matrix $\boldsymbol{\Theta}_h^+$. The next step includes the removal of dropped satellites from the current shell and the entry of the remaining satellites into the upper shell. These two dynamics are respectively represented by $\boldsymbol{\Theta}_r^-$ and $\boldsymbol{\Theta}_r^+$. Once the satellites reach their end of life, they undergo PMD and start to decrease their altitude until reentry. The satellites leaving the current shell are represented by $\boldsymbol{\Theta}_d^-$, while those entering the shell are represented by $\boldsymbol{\Theta}_d^+$. Moreover, the current model introduces a new term representing the possibility of failure during orbit transfer maneuvers ($P_{r,d}$). As for the post-mission disposal, those satellites failing in performing the maneuver transition into the derelict category. Finally, the orbit transfer flux $\dot{\boldsymbol{F}}_{ot,Q}$ for each species is expressed in Eq. (7). The orbit transfer flux and the atmospheric drag flux are summed to compute the total flux affecting the species $\dot{\boldsymbol{F}} = \dot{\boldsymbol{F}}_{ot} + \dot{\boldsymbol{F}}_d$.
In summary, Table 1 explicitly reports the primary sources, sinks, and interactions for all the species, where $S = S_h + S_r + S_d$.

4. Results

As of September 2022, the initial population for the source-sink model is taken from the currently tracked LEO population, which comprises around 24,000 objects retrieved from the Space-Track[2] Two Line Elements catalog. Moreover, DISCOSweb[3] and CelesTrak[4] sources are used to retrieve object class and status (active or inactive). The magnitude of the low-thrust acceleration ϵ is obtained by inverting Eq. (6) and solving the resulting second order equation. To this aim, real data from the full two-line elements catalog for each Starlink and OneWeb constellation satellites has been retrieved from Space-Track[2] and utilized.

4.1. MOCAT-6RD

Figure 2 provides insight into the time and altitude evolution of the six species, with S_h and D exhibiting high population levels at 400 km, 600 km, and between 1200-1300 km. Likewise, N is primarily concentrated in the upper shells between 1200-1300 km. Moreover, the count of rocket bodies declines at lower altitudes due to the impact of collisions and drag. Furthermore, the plot indicates an increasing trend in the number of satellites launched in the first 10 years, and a decreasing trend as altitude increases due to the raising flow. Similar patterns are observable in S_d, with an increase in the first few years and convergence from higher to lower altitudes. It is worth noting that a decaying satellite must reach the first shell (200-250 km) to be deemed as decayed and removed.

4.2. Orbital Capacity

To investigate the orbital capacity, a 100-year scenario using the Jacchia-Bowman 2008 atmospheric model is considered. The Jacchia-Bowman 2008 atmospheric model, with respect

[3] https://discosweb.esoc.esa.int.
[4] https://celestrak.org.

$$\dot{F}_{ot,S_h} = \mathbf{\Theta}_h^+ \ \mathbf{T}^{-1} \ S_r \tag{7a}$$

$$\dot{F}_{ot,S_r} = -\mathbf{\Theta}_h^+ \ \mathbf{T}^{-1} \ S_r + \mathbf{\Theta}_r^+ \ \mathbf{T}^{-1} \ S_r - \mathbf{\Theta}_r^- \ \mathbf{T}^{-1} \ S_r - (1-P_r) \ \mathbf{T}^{-1} \ S_r \tag{7b}$$

$$\dot{F}_{ot,S_d} = P_m \ \mathbf{\Theta}_h^- \ \mathbf{T}^{-1} \ S_h - \mathbf{\Theta}_d^- \ \mathbf{T}^{-1} \ S_d + \mathbf{\Theta}_d^+ \ \mathbf{T}^{-1} \ S_d - (1-P_d) \ \mathbf{T}^{-1} \ S_d \tag{7c}$$

$$\dot{F}_{ot,D} = (1-P_r) \ \mathbf{T}^{-1} \ S_r + (1-P_d) \ \mathbf{T}^{-1} \ S_d \tag{7d}$$

Table 1: Interactions among the species of the MOCAT-6RD model.

	Species	S (active satellites)	D (derelicts)	N (debris)	B (rocket bodies)
$\dot{\Lambda}$	$--$	λ_S	0	0	0
$\dot{C}_{PMD}$	$--$	$-(1-P_m)\vartheta_h^- S_h$	$(1-P_m)\vartheta_h^- S_h$	0	0
$\dot{F}$	$--$	$\dot{F}_{ot,S}$	$\dot{F}_{ot,D} + \dot{F}_{d,D}$	$\dot{F}_{d,N}$	$\dot{F}_{d,B}$
$\dot{C}$	S	$-\alpha_a \phi_{s,s} S^2$	$\phi_{s,d}\delta DS$ $+\phi_{s,n}\delta NS$ $+\phi_{s,b}\delta_B BS$	$n_{f,ss}\alpha_a\phi_{s,s}S^2$ $+n_{f,sd}\phi_{s,d}\alpha SD$ $+n_{f,sn}\phi_{s,n}\alpha SN$ $+n_{f,sb}\phi_{s,b}\alpha SB$	$-\phi_{s,b}(\alpha+\delta_B)\dfrac{B^2S}{B+S}$
	D	$-\phi_{s,d}(\delta+\alpha)SD$	$-\phi_{d,d}D^2$	$n_{f,dd}\phi_{d,d}D^2$ $+n_{f,dn}\phi_{d,n}DN$ $+ n_{f,db}\phi_{d,b}DB$	$-\phi_{d,b}(1+\delta_B)BD$
	N	$-\phi_{s,n}(\delta+\alpha)SN$	$-\phi_{d,n}DN$	$n_{f,nn}\phi_{n,n}N^2$	$-\phi_{n,b}(1+\delta_B)BN$
	B	$-\phi_{s,b}(\delta_B+\alpha)\dfrac{S^2B}{B+S}$	$\phi_{d,b}\delta_B DB$ $+\phi_{n,b}\delta_B NB$ $+\phi_{b,b}\delta_B B^2$	$n_{f,nb}\phi_{n,b}NB$ $+n_{f,bb}\phi_{b,b}B^2$	$-\phi_{b,b}(1+\delta_B)B^2$

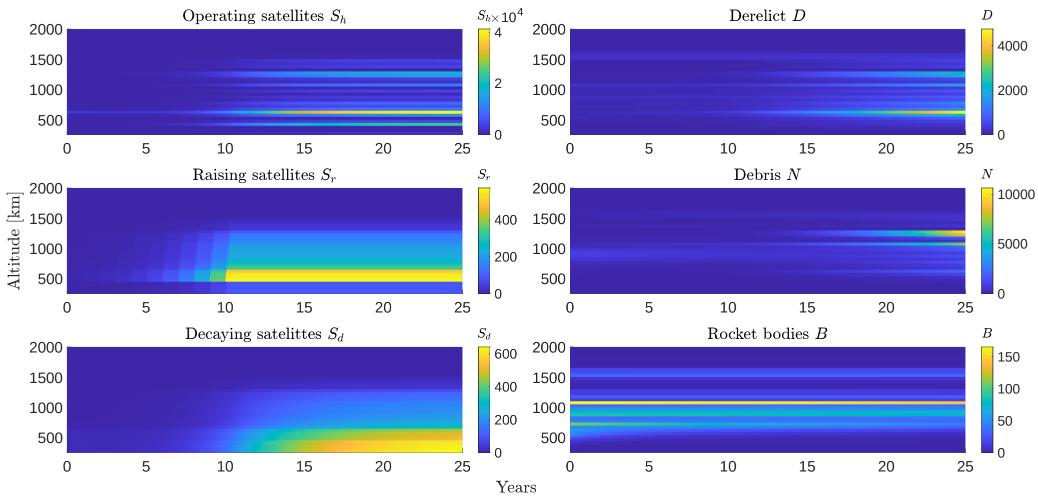

Figure 2: Population evolution in time and altitude in MOCAT-6RD model.

to the static exponential, allows to see the effects of solar cycles. The orbital capacity has been computed following Trozzi's work [2]. The number-time product and the cumulative Criticality of the Spacecraft Index (CSI) are computed. Additionally, a third metric associated to the risk of loosing satellites due to collision was defined. As an example, Figure 3 shows the cumulative CSI computed with the model considering orbit transfer maneuvers (MOCAT-6RD) and without (MOCAT-4B). It can be noted that the curve associated with rocket bodies are higher than those for derelicts, and that the curves computed with MOCAT-6RD (solid lines) are above those associated to MOCAT-4B (dashed lines).

4.3. Sensitivity Analysis

A sensitivity analysis is conducted on MOCAT-6RD to investigate the impact of varying the confidence level and the magnitude of low-thrust acceleration, while keeping all other parameters constant. To simplify computations and reduce costs, a static exponential atmospheric model

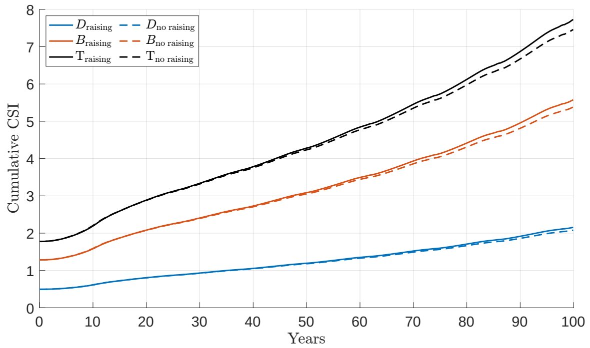

Figure 3: Cumulative CSI for MOCAT-6RD and MOCAT-4B.

is employed and the propagation time is set to 25 years. Results indicate that a higher confidence level, which corresponds to a higher number of satellites launched, leads to an increase in the number of debris and collisions. However, a lower thrust results in a decrease in the number of debris, which is not intuitive as one would expect a higher probability of collision with longer time spent in each shell. This is due to the fact that debris created at higher altitude has a longer residual lifetime than those at lower altitude. To better understand this concept, it worth to analyze Fig. 4, where three surfaces, one per species, representing the mean collision events over the altitudes and time are shown. The graph shows the total collisions involving

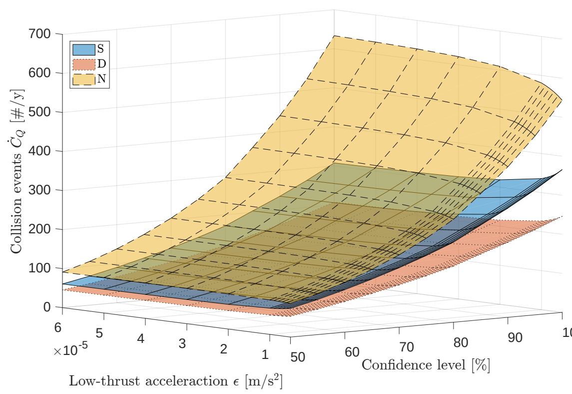

Figure 4: Collision events with a sensitivity analyses in MOCAT-6RD.

active satellites ($S = S_h + S_r + S_d$), revealing the dynamics underlying the previous analysis. A higher confidence level and lower acceleration lead to more collisions for satellites and derelicts. Lower thrust results in longer residence time while maneuvering and hence more collisions and failures. Consequently, more derelicts are created at lower altitudes with shorter lifetimes than debris. In contrast, debris created at higher altitudes remain in orbit for a longer time, increasing the orbital density and thus the probability of collisions.

4.4. Injection Orbit Altitudes Optimization

The last analysis carried out is the injection orbit altitudes optimization. The cost function is composed by three different terms: one related to the final number of active satellites in orbit, one to the final number of debris created, and one to the satellites collision events. Each term is pre-multiplied by a factor w_i, which makes the term with the same order of magnitude. The optimizations proposed consider several cost functions in which the weights w are different or equal to zero. Results indicate that using three injection orbits results in significant improvements in the final solutions. There are over 1,200 active satellites, approximately 8,200 fewer derelicts, and 3,200 fewer debris. However, there are no significant differences between the seven proposed cases, which is mainly due to the limited discretization of the altitude variations.

Figure 5 compares the solution obtained in the case with $w_{1,2} \neq 0$ and $w_3 = 0$ to the solution analyzed in Section 4.1. All solutions lead to the same reduction in derelicts and debris, but this case results in a higher number of active satellites. Including the term that maximizes the final number of operative satellites in the cost function can be advantageous for satellite-producing industries, while minimizing the final number of debris benefits both the space environment and industries.

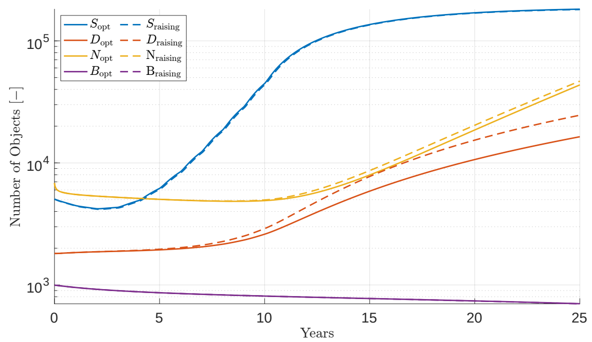

Figure 5: Comparison between the optimal and non-optimal solutions.

5. Conclusions

The thesis addressed the critical issue of space debris and the sustainability of LEO by using an evolutionary multi-shell multi-species source-sink model. The results of this study have provided valuable insights into the evolution of objects in LEO and have highlighted the importance of considering the flow of objects across multiple shells during orbit transfer maneuvers. The study develops a higher fidelity version of the MIT Orbital Capacity Assessment Tool and compares different models to show the impact of including orbit transfer maneuvers. The study also highlights the criticality of highly populated shells and reducing failures during orbit transfer maneuvers. The tool provides possibilities for further analysis and offers applications for exploring different scenarios.

References

[1] Gian Luigi Somma. *Adaptive remediation of the space debris environment using feedback control*. PhD thesis, University of Southampton, 2019.

[2] V Trozzi, C Colombo, M Trisolini, et al. Analysis of possible definitions of the space environment capacity to pursue long-term sustainability of space activities. In *INTERNATIONAL ASTRONAUTICAL CONGRESS: IAC PROCEEDINGS*, pages 1–14, 2021.

[3] Andrea D'Ambrosio, Miles Lifson, and Richard Linares. The capacity of low earth orbit computed using source-sink modeling. *arXive*, 2022. Accessed: 2022-09-6.

[4] Andrea D'Ambrosio, Simone Servadio, Peng Mun Siew, and Richard Linares. A novel source-sink model for space environment evolution with orbit capacity assessment. *Journal of Spacecraft and Rockets*, 2023.

[5] P. Krisko. Proper implementation of the 1998 nasa breakup model. *Orbital Debris Quarterly News*, 15(4):1–10, 2011. Accessed: 2022-09-14.

[6] Marilena Di Carlo and Massimiliano Vasile. Analytical solutions for low-thrust orbit transfers. *Celestial Mechanics and Dynamical Astronomy*, 133(7):1–38, 2021.